Swing Leg Control for Efficient and Repeatable Biped Walking to Emulate Biological Mechanisms

Takayuki Kawabe, Takuma Honda, and Takafumi Koseki
Department of Electrical Engineering and Information Systems, School of Engineering
The University of Tokyo, 7-3-1 Hongo, Bunkyo-Ku, Tokyo, Japan
Email: t_kawabe@koseki.t.u-tokyo.ac.jp

***Abstract*—This paper presents a energy efficient swing leg control method based on biological structures in the swing phase. In this method, structural features and the activation pattern of muscles are taken into account.**

An electromyogram result of human walking indicates that humans use the passive and active mode change and also they have typical activation pattern of muscles, especially hamstrings. Hamstrings are a pair of bi-articular muscles of a lower limb. The straight line relationship connected between hip and ankle joint is derived from structural features of this muscles. This relationship is incorporated into muscle-based landing position control in order to achieve more intuitive and effective control.

Finally, the effectiveness of the proposed control method is evaluated by comparison with a conventional walking control in a numerical case study.

I. Introduction

Technologies for humanoid robots which is based on conventional structures and control methods have been greatly advancing recently. On the other hand, some researchers who study biology and medical science indicate that there are many differences between conventional robots and humans. For that reason, biological subjects have been focused on to make a breakthrough. As a typical example, humans have bi-articular muscles which connect two joints and generate contractive force simultaneously. It is said that bi-articular muscles have been played an important role in human [1] and robot [2] motion control.

In this paper, human-like landing position control is proposed. The standard control method in the swing phase is to control each joint angle to track a given continuous trajectory with feedback control. By contrast, humans do not have a leg trajectory and use feedback signals (except for visual information) because humans have these system inside their muscles. The proposed method only uses bi-articular muscle signals with simplified musculoskeletal structures. The approach is based on antagonistic muscle control proposed by N. Hogan [3] and K. Ito et al., [4]. In addition, K. Yoshida et al., demonstrated this control method with bi-articular muscle [5]. However, these studies were only applied for a robotic arm and did not mention passivity and biological structures excluding antagonistic muscles. The most important characteristic of human walking is high energy efficiency. P. Kormushev et al., experimentally archieved the biped walking energy minimization with actual springs [6]. D. P. Ferris et al., claimed that humans modulate the viscoelasticity during environmental interaction [7]. As well as these studies, the authors focused on the modulation of muscle viscoelasticity from the point of view of mono- and bi-articular muscles coactivation. In addition to that, simple landing position control should be designed for practical use. Therefore, the authors proposed intuitive landing point design method modulating muscle viscoelasticity for the purpose of human-like energy efficient walking.

First, human's muscle activity is investigated, especially in bi-articular muscles which is called "hamstrings". The authors emphasize this muscle works to realize both high energy efficiency and simple landing position control in the swing phase. Second, the authors mention the intuitive design method of landing position and how to vary the leg viscoelasticity is discussed. Finally, the effectiveness of the proposed control method is evaluated by simulations.

II. The Investigation of Muscle Activity During the Swing Leg Action

Fig. 1 shows the effective muscle model [1] which is simplified muscle activity of a lower limb. Note that bi-articular muscles, the main interest of our approach, are mainly located in sagittal plane, therefore the following study have been discussed in this sagittal plane model.

As a next step, details of muscle activation have been examined. According to an electromyogram (EMG) of a lower

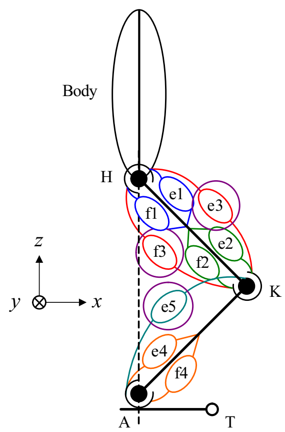

Fig. 1. Effective muscle model of a lower limb. ("e" and "f" mean extensor and flexor muscle.)

limb while walking [8] [9], Tibialis anterior, Extensor hallucis longus, and Extensor digitorum longus (f5) have been activated at all times in the swing phase. Contrary to this, (e4) (e.g. Gastrocnemius) and (e5) (e.g. Soleus) muscles have not been activated little or nothing at all. It seems reasonable to consider that muscles around ankle only need to act in order to flex their foot until the end of the swing phase. These muscles do not influence to general tendency of the swing leg. For that reason, the part of their feet has been removed in the following study.

Here, the authors divide the swing phase into two parts. The first part of the swing phase, muscle activity is also simple. Iliacus, psoas major (e1), and rectus femoris (e3) act to swing their leg. It has been reported that the duration of muscle activity becomes longer when walking speed increase [9]. After this swing action, only a little muscle activity have been observed for a while, that is to say practically passive. Humans do not need muscle activation under the condition that a tip of swing leg must not strike on the ground. Generally, humans can satisfy this condition if their leg is swung at the first part of the swing phase because their knee is automatically flexed by inertial effect of the lower limb.

In the latter part of the swing phase, particularly active muscles are hamstrings (f3) which includes Biceps femoris, Semimembranosus, and Semitendinosus. Vastus medialis (e2) is also activated strongly. Other active muscles are psoas (e1), vastus lateralis (e2), popliteus (f2), gluteus maximus, and gluteus medius (f1). It should be noted that this assumption does not mean characteristics common to all. There are some individual differences and walking speed dependence [10]. Nevertheless, the essential combination of muscles such as hamstrings have been observed from some EMG data.

One of the objectives of this study is how to decide the landing position at the end of the swing phase. It is clear that humans do not have precise landing position in their mind. However, they can adjust the landing position when they find an unexpected obstacle. The authors focused on hamstrings activity because humans might have some control laws in the latter part of the swing phase, as a result of EMG data.

III. VISCOELASTIC MODEL OF MUSCLE

The following approach is based on the approximate formula of nonlinear muscle model, as shown in Fig. 2 [4].

$$F = u - kux - bu\dot{x} \tag{1}$$

In (1), F is total muscle force, u is muscle contraction unit, x is the length of muscle which is defined as relative displacement from the natural length l_0, k is the elastic coefficient, and b is the viscous coefficient. Humans have antagonist muscles in each joint. For that reason, (1) is expressed as (2).

$$F = (u_f - u_e) - k(u_f + u_e)x - b(u_f + u_e)\dot{x} \tag{2}$$

In (2), subscripts f and e denote flexor and extensor muscle. In short, humans can adjust u_f and u_e to obtain the desired impedance characteristics.

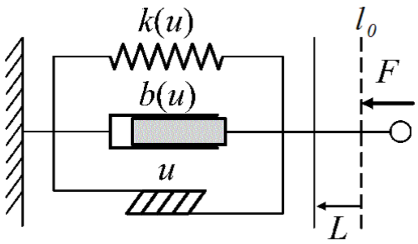

Fig. 2. Muscle viscoelastic model.

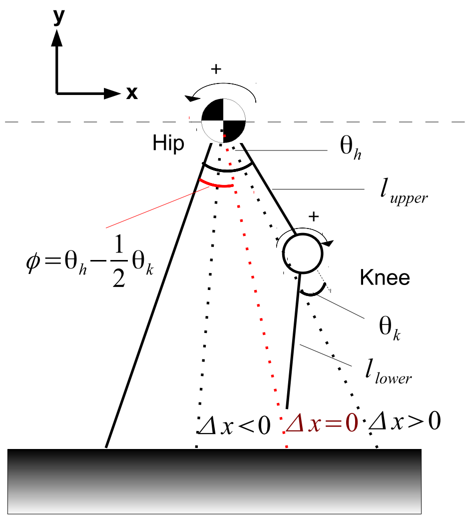

Fig. 3. The influence of muscle length deviation in hamstrings.

IV. THE STRAIGHT LINE RELATIONSHIP REPRESENTED BY HAMSTRINGS

According to the previous section, hamstrings (f3) especially act in the latter part of the swing phase. Here, the authors describe why humans choose hamstrings instead of other redundant muscles. Output force of hamstrings, as shown in (3), can be derived from (2) and the length of moment arm r which is the distance from a muscle's line of action to the joint's center of rotation.

$$F = u - ku(r_h\theta_h - r_k\theta_k) - bu(r_h\dot{\theta}_h - r_k\dot{\theta}_k) \tag{3}$$

In (3), θ is angle of each joint defined by Fig. 3 and subscripts "h" and "k" denote "Hip" and "Knee". Note that θ should be written in the displacement from the natural angle θ_0 which is defined by the natural length of muscle l_0. This time, however, the natural angle is set to zero for convenience.

Here, the moment arm length r of hamstrings is focused. In case of Rectus femoris (e3), both side of the length of moment arm r_h and r_k is almost the same [8]. By contrast, in case of hamstrings (f3), the length of moment arm of hip is about twice as long as that of knee. The length of moment arm is generally vary with angle, however this relationship is almost satisfied in the swing phase [11].

If this relationship is adopted, the ratio of moment arm is $r_h : r_k = 2 : 1$ in hamstrings. The joint torque of hip (T_h) and knee (T_k) are described as (5) and (6).

$$
\begin{aligned}
F &= u - kur(\theta_h - \frac{1}{2}\theta_k) - bur(\dot{\theta}_h - \frac{1}{2}\dot{\theta}_k) && (4)\\
T_h &= -r\{u - kur(\theta_h - \frac{1}{2}\theta_k) - bur(\dot{\theta}_h - \frac{1}{2}\dot{\theta}_k)\} && (5)\\
T_k &= \frac{1}{2}r\{u - kur(\theta_h - \frac{1}{2}\theta_k) - bur(\dot{\theta}_h - \frac{1}{2}\dot{\theta}_k)\} && (6)
\end{aligned}
$$

It is reasonable that muscle force effects hip joint stronger than knee joint because the lower part of a leg can be moved easily.

If the length of each link is the same as humans, $\phi = \theta_h - \frac{1}{2}\theta_k$ can be expressed as the straight line which connects hip joint and knee joint. As shown in Fig. 3, this relationship looks like a simplified compasses model. $\Delta x = r\Delta\phi$ denotes deviation of hamstrings length from the natural length l_0. Given that the value of Δx becomes large, feedback terms described in (5) and (6) also increase in order to reduce deviations.

Thus, this relationship implies that humans use hamstrings to employ the straight line relationship between hip and knee joint.

V. Mathematical examination of muscle activation patterns

It is necessary to incorporate antagonistic activation to set the landing position. From (2), it can be balanced $(u_f - u_e)$ with $k(u_f + u_e)x$ at an equilibrium point. For that reason, u_f and u_e should be adjusted to set given point.

For example, antagonistic muscles work in the plane surface without any disturbance [4] [5]. Joint torque can be expressed as (7).

$$T = r(u_f - u_e) - kr^2(u_f + u_e)\theta - br^2(u_f + u_e)\dot{\theta} \qquad (7)$$

In steady-state condition, $\dot{\theta}$ and $\ddot{\theta}$ become zero. Hence, θ is given by (8).

$$\theta = \frac{u_f - u_e}{kr(u_f + u_e)} \qquad (8)$$

That is, the ratio of u_f and u_e defines the angle of equilibrium point.

According to the previous section, humans do not use all their muscles simultaneously. Let us suppose the case (f3), (e1), and (e2) muscles act antagonistically. Here, a biped model shown in Fig. 4 is used.

A. Muscle activation model in the swing phase

At first, the non-linear equation of the biped walking model is taken into account, especially gravity effects. d_i consisting of non-linear equation of motion and disturbance is introduced for the moment. In steady-state condition, $\dot{\theta}_2$, $\ddot{\theta}_2$, $\dot{\theta}_3$, and $\ddot{\theta}_3$ are set to zero. Hence, major components of d_i are interference term of $\ddot{\theta}_1$ and gravity term. In conventional robots, precise position tracking can be achieved by suppressing the effects of d_i. On the other hand, passivity based robots achieve high energy efficiency by employing the effects of d_i. The authors have emphasized that humans have both advantages. It is shown in following analysis.

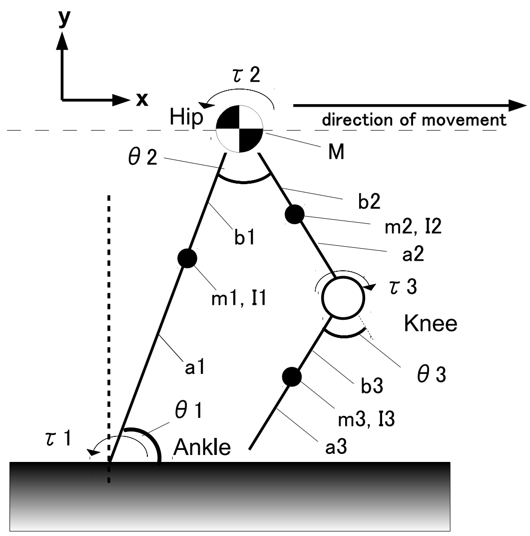

Fig. 4. The biped walking model.

The length of moment arm r, elastic coefficient k, and viscous coefficient b for each muscle are regarded as the same value for simplicity. Most important characteristics are that bi-articular muscle (f3) acts two adjacent joints with different length of moment arm. In case of mono-articular muscles, this difference will be corporated into muscle contraction units u_i.

If (f3), (e1), and (e2) muscles act antagonistically, joint torques are described in (9) and (10).

$$
\begin{aligned}
T_2 &= (ru_2 - ru_{23}) - r^2ku_2\theta_2 - r^2ku_{23}(\theta_2 - \frac{1}{2}\theta_3)\\
&- r^2bu_2\dot{\theta}_2 - r^2bu_{23}(\dot{\theta}_2 - \frac{1}{2}\dot{\theta}_3) + d_2 && (9)\\
T_3 &= (\frac{1}{2}ru_{23} - ru_3) - r^2ku_3\theta_3 + \frac{1}{2}r^2ku_{23}(\theta_2 - \frac{1}{2}\theta_3)\\
&- r^2bu_3\dot{\theta}_3 + \frac{1}{2}r^2bu_{23}(\dot{\theta}_2 - \frac{1}{2}\dot{\theta}_3) + d_3 && (10)
\end{aligned}
$$

In (9) and (10), u_{23} is the muscle contraction unit of hamstrings (f3), u_2 is that of hip extensor muscles (e1), and u_3 is that of knee extensor muscles (e2).

The equilibrium point in steady-state condition is expressed as (11) and (12).

$$\theta_2 = \frac{\{(u_3 + \frac{1}{4}u_{23})D_2 + \frac{1}{2}u_{23}D_3\} + \{(u_3 + \frac{1}{4}u_{23})\frac{d_2}{r} + \frac{1}{2}u_{23}\frac{d_3}{r}\}}{rk\{(u_3 + \frac{1}{4}u_{23})u_2 + \frac{1}{2}u_{23}(2u_3)\}} \qquad (11)$$

$$\theta_3 = \frac{\{\frac{1}{2}u_{23}D_2 + S_2D_3\} + \{\frac{1}{2}u_{23}\frac{d_2}{r} + S_2\frac{d_3}{r}\}}{rk\{\frac{1}{2}u_{23}(\frac{1}{2}u_2) + S_2u_3\}} \qquad (12)$$

In (11) and (12), $D_2 = u_2 - u_{23}, S_2 = u_2 + u_{23}, D_3 = \frac{1}{2}u_{23} - u_3, S_3 = \frac{1}{2}u_{23} + u_3$. In this case, the equilibrium point is set by antagonistic muscles in arbitrary. The effects from d_i can be suppressed if muscle contraction units u_i increase. It is like a exerting full strength of human's motion.

TABLE I
THE MATH VARIABLES IN A BIPED WALKING MODEL FOR A CASE STUDY.

symbol	value	symbol	value
a_1 (m)	0.47	b_1 (m)	0.33
a_2 (m)	0.20	b_2 (m)	0.20
a_3 (m)	0.20	b_3 (m)	0.20
M (kg)	40.0	m_1 (kg)	4.8
m_2 (kg)	3.2	m_3 (kg)	1.6
$I_1(\mathrm{kgm}^2)$	0.2571	$I_2(\mathrm{kgm}^2)$	0.0434
$I_3(\mathrm{kgm}^2)$	0.0217	$r(m)$	0.03

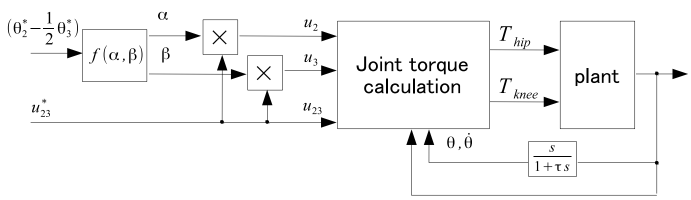

Fig. 5. Block diagram of the proposed method. ($f(\alpha, \beta)$ denotes the ratio of muscle contraction force calculated by (15) and (16).)

There are two equations (11) and (12) compared with three variables, therefore $\alpha = \frac{u_2}{u_{23}}$, $\beta = \frac{u_3}{u_{23}}$ are given for replacement, as shown in (13) and (14).

$$\theta_2 = \frac{(\beta + \frac{1}{4})(\alpha - 1 + \frac{1}{u_{23}}\frac{d_2}{r}) + \frac{1}{2}(\frac{1}{2} - \beta + \frac{1}{u_{23}}\frac{d_3}{r})}{rk(\alpha\beta + \frac{1}{4}\alpha + \beta)} \tag{13}$$

$$\theta_3 = \frac{\frac{1}{2}(\alpha - 1 + \frac{1}{u_{23}}\frac{d_2}{r}) + (\alpha + 1)(\frac{1}{2} - \beta + \frac{1}{u_{23}}\frac{d_3}{r})}{rk(\alpha\beta + \frac{1}{4}\alpha + \beta)} \tag{14}$$

Here, θ_2^* and θ_3^* are used as reference equilibrium points. On the assumption that u_{23} has larger value, (13) and (14) can be expressed as (15) and (16) using $\Theta_i = rk\theta_i^*$.

$$\alpha = \frac{1 + \Theta_2 - \frac{1}{2}\Theta_3}{1 - \Theta_2} \tag{15}$$

$$\beta = \frac{1 + \Theta_2 - \frac{1}{2}\Theta_3}{2(1 + \Theta_3)} \tag{16}$$

α and β can be uniquely specified if reference equilibrium points are given. u_{23} is freely chosen as a coefficient of total muscle intensity to suppress the effects of d_i.

According to human walking, the muscle contraction intensity of hamstrings u_{23} gradually increases during the end of the swing phase. If the effects of d_i become larger, the swing leg is practically moved by passive dynamics with low actuator torques. If the effects of d_i become smaller, the swing leg is moved by actuator torques with precise control. It means that humans can switch the control mode between "passive" and "active" gradually by using u_{23}.

VI. PARAMETER DETERMINATION FOR THE SIMULATION

In this section, actual muscle values are estimated for the simulation. The biped walking model is shown in Fig. 4 and Table I. The simulation was conducted in the initial posture θ_1 = 110 deg, θ_2 = -30 deg, θ_3 = 15 deg. MATLAB/simulink have been employed for the simulation. The details of walking model such as an upper limb and feet are removed for simplicity.

As mentioned above, humans do not have the landing point consciously and there is no accurate control in the first part of the swing phase. For that reason, the hip joint torque is simply given to swing the leg in that time. For example, $T_2 = k\dot{\theta}_1$ which is proportional to $\dot{\theta}_1$ with low pass filter to smooth the input torque. Besides, the stance leg illustrated in Fig. 4 is not actuated. It is driven by initial velocity $\dot{\theta}_1$ and passive dynamics.

The block diagram of the proposed method is shown in Fig. 5. Reference values are muscle contraction force of hamstrings u_{23} and landing angle of hamstrings $(\theta_2 - \frac{1}{2}\theta_3)^*$. According to a landing posture of stable walking of humans, the knee angle θ_3^* is always extended. For this reason, the reference value of θ_3^* is set to the fixed value $\theta_3^* = -60$ deg. It means that θ_2^* is needed to set the landing point, but it is more natural to think the direction of straight line characteristics $(\theta_2 - \frac{1}{2}\theta_3)^*$.

A. Natural length l_0 and viscoelastic coefficients k, and b

Here, the natural angle θ_n is defined as the joint angle when the muscle length is natural l_0. It is the intermediary position of joint moving range in general, θ_{2n} = 55 rad and θ_{3n} = 65 rad. The authors have considered how θ_n effects to the walking motion.

Let us suppose that the target landing position is given as θ = p in Fig. 4. It means the reference value is given by θ^* = p - θ_n. If the natural angle θ_n changes, it is equivalent to change the reference angle θ^*. From (15) and (16), the ratio of muscle contraction α, β is varied by θ^*. When the value of θ_2^* becomes large or θ_3^* becomes small, α and β also become large. In other words, the reference straight line angle $(\theta_2 - \frac{1}{2}\theta_3)^*$ is stepped forward, the intensity of muscle contraction becomes stronger simultaneously. This is an advantage of considering the natural angle because the effect of gravity term is getting higher together with the value of $(\theta_2 - \frac{1}{2}\theta_3)^*$ that being said gravity effect can be suppressed by stronger muscle contraction force automatically.

Viscoelastic coefficients k and b have been also estimated. From (2), real viscoelasticity of joints includes summation of antagonistic muscle contraction units. For that reason, it is difficult to measure the actual value of viscoelastic coefficients. However, the maximum value of k is limited on the condition that u_i must be positive in (13) and (14). As a result, k should be smaller than 30 N/m. In addition, the ratio of elasticity and viscosity is not influenced by muscle contraction units. For that reason, b can be estimated by k. $k = 10$ N/m and $b = 1.3$ Ns/m are used in this simulation.

B. Muscle contraction force of hamstrings u_{23}

From human's EMG pattern, u_{23} is proportional to time. It means that effective viscoelastic coefficients $k' = ku_i$ and b' = bu_i will be larger in order to change transient characteristics. If u_{23} is increased proportionally, transient characteristics of θ_i also change under-damped to over-damped because effective k' and b' increase in the same ratio. In addition, the effect

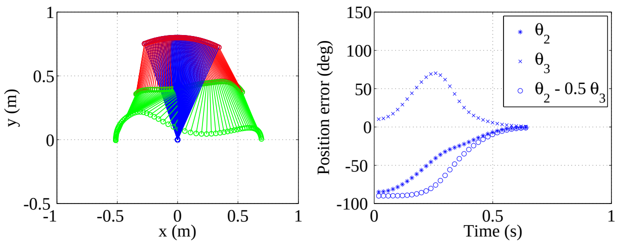

(a) stick diagram (b) position errors

Fig. 6. Stick diagram and angle errors in case (I).

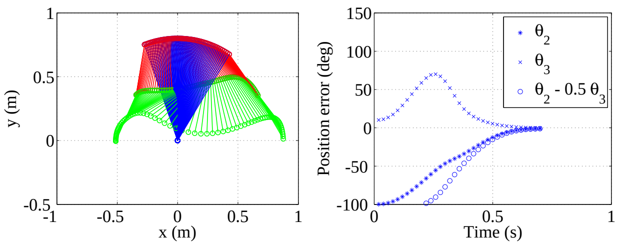

(a) stick diagram (b) position errors

Fig. 7. Stick diagram and angle errors in case (II).

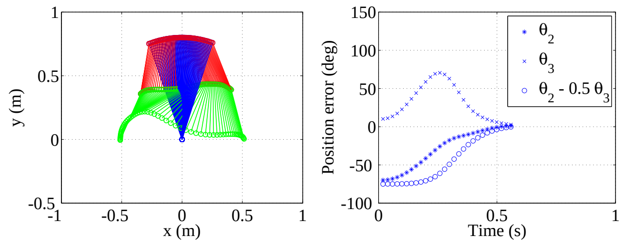

(a) stick diagram (b) position errors

Fig. 8. Stick diagram and angle errors in case (III).

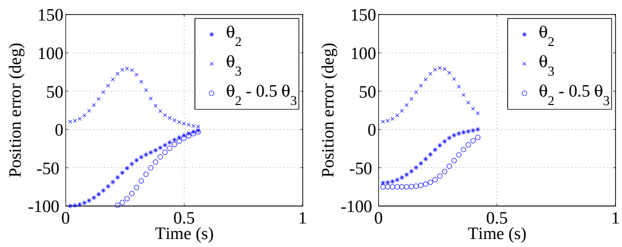

(a) case (IV) (b) case (V)

Fig. 9. Position errors when v = 1.2 m/s.

of d_i can be suppressed gradually, therefore u_{23} changes the mode "passive" to "active" as mentioned above sections.

Time variable u_{23} is approximated, as shown in (17).

$$u_{23} = a(t - t_0) \tag{17}$$

In (17), a is the coefficient of intensity, t is time and t_0 is initial time. In following simulation, the authors have determined $a = 1.0 \times 10^4$ and $t_0 = 0.2$ sec (about the middle of the swing phase).

VII. Numerical Study for Evaluation of Proposed Method

A. Followability of the reference position

Generally, the most efficient walking speed is about v = 1.0 - 1.5 m/s [12]. Here, the walking speed is given by v = 1.0 m/s for each pattern. In the simulation, the authors have considered in the following three cases.

(I) Reference value is set to $(\theta_2^* - \frac{1}{2}\theta_3^*)$ = 30 deg. (A stick diagram and position errors are illustrated in Fig. 6.)

(II) Reference value is set to $(\theta_2^* - \frac{1}{2}\theta_3^*)$ = 45 deg. (A stick diagram and position errors are illustrated in Fig. 7.)

(III) Reference value is set to $(\theta_2^* - \frac{1}{2}\theta_3^*)$ = 15 deg. (A stick diagram and position errors are illustrated in Fig. 8.)

As a result, position errors were nearly zero in all patterns. Therefore, the effects of d_i have been suppressed sufficiently.

B. Robustness under variable walking speeds v

Here, walking speed v is increased to $v = 1.2$ m/s.

(IV) Reference value is set to $(\theta_2^* - \frac{1}{2}\theta_3^*) = 45$ deg, position errors are illustrated in Fig. 9(a).

(V) Reference value is set to $(\theta_2^* - \frac{1}{2}\theta_3^*) = 15$ deg, position errors are illustrated in Fig. 9(b).

In the case of (V), position errors are left to some extent. This is because there is not enough settling time and the swing leg collide to the ground before errors are settled. For this reason, it is necessary to set the landing point to a distant place when walking speed is increased. However, it is same as the case of human walking. If humans walk more high speed, walking step needs to be enlarged [12].

As a result, there are some constraint on walking speed and walking step. It is necessary to change the muscle contraction ratio α and β to move the landing point farther.

C. Energy efficiency

The proposed control method is evaluated through comparison with conventional control method. In conventional method, joint angles θ_2 and θ_3 are set to the reference angle by PD controller. In order to evaluate under the same condition, PD gain is given by effective viscoelastic values in steady-state condition in case (I). Simulation conditions are the same as case (I) except for the control methods.

Position errors are illustrated in Fig. 10. Position errors are reduced quickly in the conventional method. However, passivity is sacrificed and steady-state errors are almost the same level as the proposed method. For that reason, there is no practical difference between them.

Input torques in the proposed and conventional methods are illustrated in Fig. 11. Comparing with the conventional method, peak torques are decreased in the proposed method, it is useful for reducing actuator size.

In addition, evaluation values of total energy consumption $(= \int |\tau\omega| dt)$ are illustrated in Fig. 12. Total energy consump-

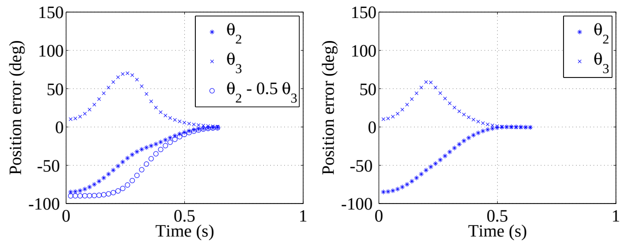

(a) the proposed method (b) the conventional method

Fig. 10. Position errors in the proposed and conventional methods.

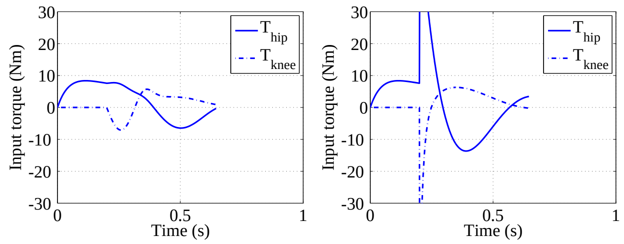

(a) the proposed method (b) the conventional method

Fig. 11. Input actuator torques in the proposed and conventional methods.

tion in the proposed method is about 50% less than that in a conventional one.

Therefore, it has been cleared that landing position control with high energy efficiency can be achieved by the proposed method.

VIII. Conclusion

The authors have proposed a swing leg control method based on biological mechanisms and evaluated in advantages of better energy efficiency. Structure and patterns of muscle activation in biological legs were taken into account. A typical pattern of muscle activation has been observed from EMG waveforms, which implies the hamstrings play a major role in the motion in the swing phase.

Biological structure of lower limb and antagonistic muscles are significant in the muscle-based control for simplifying activation patterns. The proposed control method is based on the length and muscle contraction intensity of hamstrings. The length of hamstrings contributes to the intuitive design of the landing position with the straight line relationship. The muscle contraction intensity of hamstrings also contributes to the variation of the leg viscoelasticity. A repeatable and stable biped walking motion is possible by using passive dynamics according to the proposed control method.

A case study has been numerically calculated to verify the expected advantages of the proposed method, i.e, high energy efficiency and landing position control assuming dimensions and structure identical to a human body. As a result, energy consumption of the proposed method could be reduced by 50% compared with that in a conventional one.

The numerical results have suggested the following problems to be improved in further studies. The proposed control

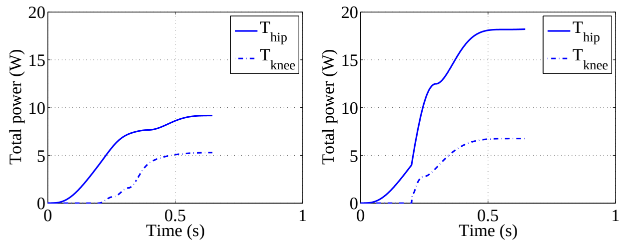

(a) the proposed method (b) the conventional method

Fig. 12. Evaluation values of total energy consumption in the proposed and conventional methods.

method shall be applied to an experimental bench. The proposed activation pattern is valid just in slower walking motion. The EMG measurement shows different, more complicated activation patterns for faster motions. Therefore, it will be difficult to determine parameters because of redundancy of muscles. In addition, muscle activation patterns in the stance phase and touch-down phase are very important from the point of view of energy saving walking. The proposed method should be expanded for practical use.

References

[1] M. Kumamoto, “Evolution of motion control, revolution in humanoid robots,” Tokyo denki university press, 2006.

[2] V. Salvucci, Y. Kimura, S. Oh, and Y. Hori, “Force maximization of biarticularly actuated manipulators using infinity norm,” IEEE/ASME Transactions on Mechatronics, 2012.

[3] N. Hogan, “Adaptive control of mechanical impedance by coactivation of antagonist muscles,” IEEE Transactions on automatic control, Vol. AC-29, No. 8, 1984.

[4] K. Ito, and T. Tsuji, “The bilinear characteristics of muscle skeletomotor system and the application to prosthesis control,” The Transactions of Electrical Engineers of Japan 105-C, No.10, pp. 201-206, 1985.

[5] K. Yoshida, T. Uchida, and Y. Hori, “Novel FF Control algorithm of robot arm based on bi-articular muscle principle emulation of muscular viscoelasticity for disturbance suppression and path tracking,” Proc. of Annual Conference of the IEEE Industrial Electronics Society, pp. 310-315, 2007.

[6] P. Kormushev, B. Ugurlu, S. Calinon, N. G. Tsagarakis, and D. Caldwell, “Bipedal walking energy minimization by reinforcement learning with evolving policy parameterization,” Proc. of International Conference on Intelligent Robots and System, San Francisco, US, pp. 318-324, 2011.

[7] D. P. Ferris, M. Louie, and C. T. Farley, “Running in the real world: Adjusting leg stiffness for different surfaces,” Proc. of Royal Society London, vol. 265, pp. 989-993, 1998.

[8] Irving P. Herman, “Physics of the human body,” Springer, 2007.

[9] E. A. Andersson, J. Nilsson, and A. Thorstensson, “Intramuscular EMG from the hip flexor muscles during human locomotion,” Acta Physiol Scand, 161, pp. 361-370, 1997.

[10] H.J.A. van Hedel, L. Tomatis, and R. Muller, “Modulation of leg muscle activity and gait kinematics by walking speed and bodyweight unloading,” Gait Posture 24, 35-45, 2006.

[11] A. S. Arnold, S. Salinas, D. J. Asakawa, and S. L. Delp, “Accuracy of muscle moment arms estimated form MRI-based musculoskeletal models of the lower extremity,” Computer Assisted Surgery, Vol. 5, pp. 108-119, 2000.

[12] Y. Goto, K. Matsushita, K. Honma, A. Tsujino, and T. Okamoto, “Electromyographic study of walking pattern in relation to speed,” Annals of physical education, No.13, pp. 39-52, 1978.